Assessment of Bromodomain Target Engagement by a Series of BI2536 Analogues with Miniaturized BET-BRET

Luke W. Koblan+,[c] Dennis L. Buckley+,[a, b] Christopher J. Ott+,[a, b, c] Mark E. Fitzgerald+,[c, h] Stuart W. J. Ember,[d, g] Jin-Yi Zhu,[d] Shuai Liu,[e] Justin M. Roberts,[a] David Remillard,[a] Sarah Vittori,[a, c] Wei Zhang,[e] Ernst Schonbrunn,[d] and James E. Bradner*[a, b, c, f]

Evaluating the engagement of a small molecule ligand with a protein target in cells provides useful information for chemical probe optimization and pharmaceutical development. While several techniques exist that can be performed in a low-throughput manner, systematic evaluation of large compound libraries remains a challenge. In-cell engagement measurements are especially useful when evaluating compound classes suspected to target multiple cellular factors. In this study we used a bioluminescent resonant energy transfer assay to assess bromodomain engagement by a compound series containing bromodomain- and kinase-biasing polypharmacophores based on the known dual BRD4 bromodomain/PLK1 kinase inhibitor BI2536. With this assay, we discovered several novel agents with bromodomain-selective specificity profiles and cellular activity. Thus, this platform aids in distinguishing molecules whose cellular activity is difficult to assess due to polypharmacologic effects.

Bromodomains are highly conserved protein modules that recognize post-translationally modified ε-acetylated lysine resi-

[a] Dr. D. L. Buckley,+ Dr. C. J. Ott,+ J. M. Roberts, D. Remillard, S. Vittori, Prof. Dr. J. E. Bradner
Department of Medical Oncology, Dana-Farber Cancer Institute, Boston, MA 02215 (USA)
E-mail: james_bradner@dfci.harvard.edu

[b] Dr. D. L. Buckley,+ Dr. C. J. Ott,+ Prof. Dr. J. E. Bradner
Department of Medicine, Harvard Medical School, Boston, MA 02115 (USA)

[c] L. W. Koblan,+ Dr. C. J. Ott,+ Dr. M. E. Fitzgerald,+ S. Vittori, Prof. Dr. J. E. Bradner
Center for the Science of Therapeutics, Broad Institute, Cambridge, MA 02142 (USA)

[d] Dr. S. W. J. Ember, Dr. J.-Y. Zhu, Prof. Dr. E. Schonbrunn
Drug Discovery Department, Moffitt Cancer Center, Tampa, FL 33612 (USA)

[e] S. Liu, Prof. Dr. W. Zhang
Department of Chemistry, University of Massachusetts-Boston, Boston, MA 02125 (USA)

[f] Prof. Dr. J. E. Bradner
Current address: Novartis Institutes for Biomedical Research, Cambridge, MA 02139 (USA)

[g] Dr. S. W. J. Ember
Current address: Reaction Biology Corporation, Malvern, PA 19355 (USA)

[h] Dr. M. E. Fitzgerald+
Current address: C4 Therapeutics, Cambridge, MA 02142 (USA)

[+] These authors contributed equally to this work.

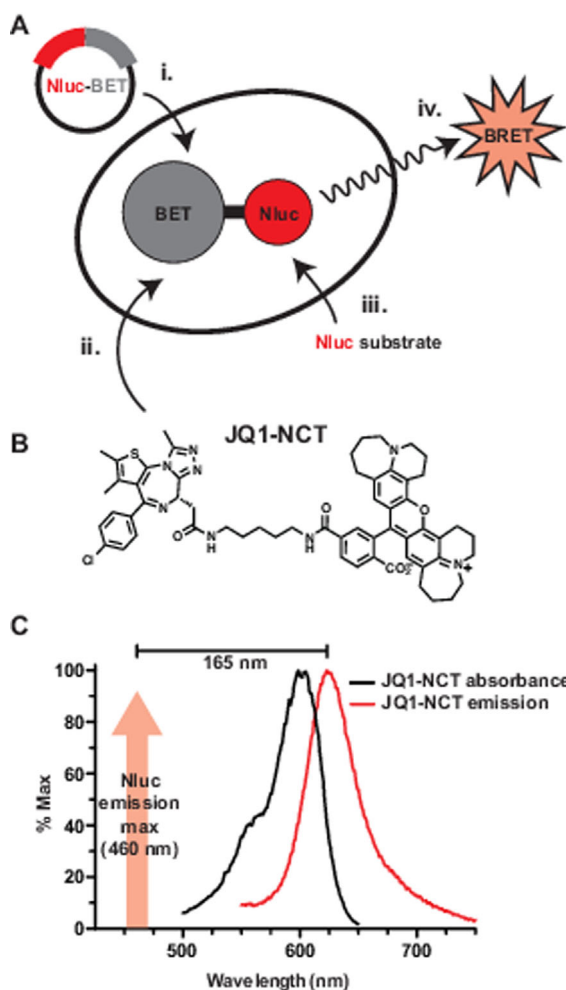Supporting information and the ORCID identification number(s) for the author(s) of this article can be found under http://dx.doi.org/10.1002/cmdc.201600502.

dues. Owing to their structurally distinct hydrophobic acetyllysine recognition pocket, bromodomains have proven tractable targets for synthetic small-molecule ligand development.[1] The first reported bromodomain inhibitors were shown to potently and selectively displace the bromodomain-and-extra terminal domain (BET) family bromodomains from acetyllysine-bearing histone peptides in vitro and from regions of acetylated chromatin in cells.[2–4] The BET bromodomain protein family has four members—BRD2, BRD3, BRD4, and BRDT—each involved in a number of biological processes including epigenetic regulation and control of gene expression. Since the original publication of BET bromodomain ligands, a variety of inhibitors with diverse scaffolds have been developed with several being studied in clinical trials for indications such as cancer and cardiovascular disease.[5–9] Pre-clinical development of these inhibitors has been enabled by a number of cell-free in vitro assays for compound hit discovery and lead optimization; however, the typical assays for assessing cellular compound activity, including fluorescence recovery after photo-bleaching (FRAP) and chromatin immunoprecipitation (ChIP), are much lower throughput and can suffer from poor dynamic range. In fact, general and robust high-throughput methods to determine ligand association with target proteins in live cells are not thoroughly used. Fluorescence or bioluminescence resonance energy transfer (FRET/BRET) systems with paired energy donors and acceptors can be used to detect protein–protein and protein–ligand interactions, though it can be difficult to achieve the necessary sensitivity and dynamic range required for screening assays. Here we sought to evaluate the use of a cell-permeable fluorophore-tagged BET bromodomain ligand for use in a miniaturized bioluminescence resonance energy transfer (BET-BRET) assay. This assay is based on technology recently developed by the Promega Corporation whereby the use of nanoluciferase (Nluc) as a bioluminescent BRET donor can substantially increase assay signals in live-cell protein–protein interaction studies, including BRD4 binding to histones.[10] We used this strategy for a simplified bromodomain ligand-displacement assay system by appending a fluorescent acceptor nonchloro TOM (NCT) dye onto an accessible site of JQ1, a definitive BET bromodomain probe ligand (Figure 1 A,B).[2] The NCT dye has minimal spectral overlap with Nluc, and has recently been described as an effective BRET tracer dye when conjugated to histone deacetylase and bromodomain-binding small molecule ligands.[11, 12] Thus, we considered that adaptation of this assay with a JQ1-conjugate in miniaturized screening-plate format may be a useful addition to bromodomain in-

Figure 1. BET-BRET assay design with JQ1-NCT. A) Schematic of the assay. Nluc-BET fusion proteins are transiently transfected into cells (i); cells are treated with JQ1-NCT tracer (ii); Nluc substrate is added (iii); and BRET signal is recorded (iv). B) JQ1-NCT dye structure. C) Spectral characteristics of JQ1-NCT. Nluc emission as determined in Machleidt et al.[10]

Figure 2. Evaluation of BET-BRET assay parameters with JQ1-NCT. A) Determination of optimal BET-BRET acceptor/donor ratios. A four-point titration of donor Nluc-BRD4 (full-length) plasmid with four concentrations of acceptor JQ1-NCT dye. Signal was evaluated as described in the Experimental Section. The ratio used for subsequent experiments is denoted with a red asterisk. B) Evaluation of mBRET signal across all BET family members (***$p < 0.001$, ****$p < 0.0001$). C) BET ligands of varying potencies evaluated in the BRD4 BET-BRET assay. Cells were treated at a concentration of 1 μM for 2 h. D) Evaluation of JQ1 dose–response in the BRD4 BET-BRET assay. E) 384-well Z'-factor assessment comparing two concentrations of JQ1 inhibition. Z'-factor is reported for DMSO versus 10 nM and 1000 nM JQ1. Each condition was tested with $n = 40$ samples.

hibitor development to identify JQ1-competitive compounds. The BET-BRET assay consists of transient expression of full-length BET proteins amino-terminally tagged with Nluc. The JQ1-NCT probe is added to live cells, followed by addition of the Nluc substrate furimazine to generate a BRET signal. Similar to other NCT-conjugated dye systems described by Wood and colleagues,[10–12] the JQ1-NCT probe displayed fluorescent properties that notably achieve 165 nm of spectral emission separation from the Nluc donor (Figure 1C). To characterize cellular penetration of the dye and optimal BET-BRET conditions, varying ratios of transfected Nluc-BRD4 and JQ1-NCT were evaluated (Figure 2A). Using a 96-well assay format, we found that 250 nM of JQ1-NCT produced the highest signal to background ratio at all concentrations of transfected Nluc-BRD4 tested. For subsequent experiments, a ratio of 50 ng Nluc-BET with 250 nM JQ1-NCT was selected as it generated the most consistent data. Using these conditions, JQ1-NCT generated significant BRET signal with all four members of the BET protein family (Figure 2B). Some variation in maximal signal intensity is
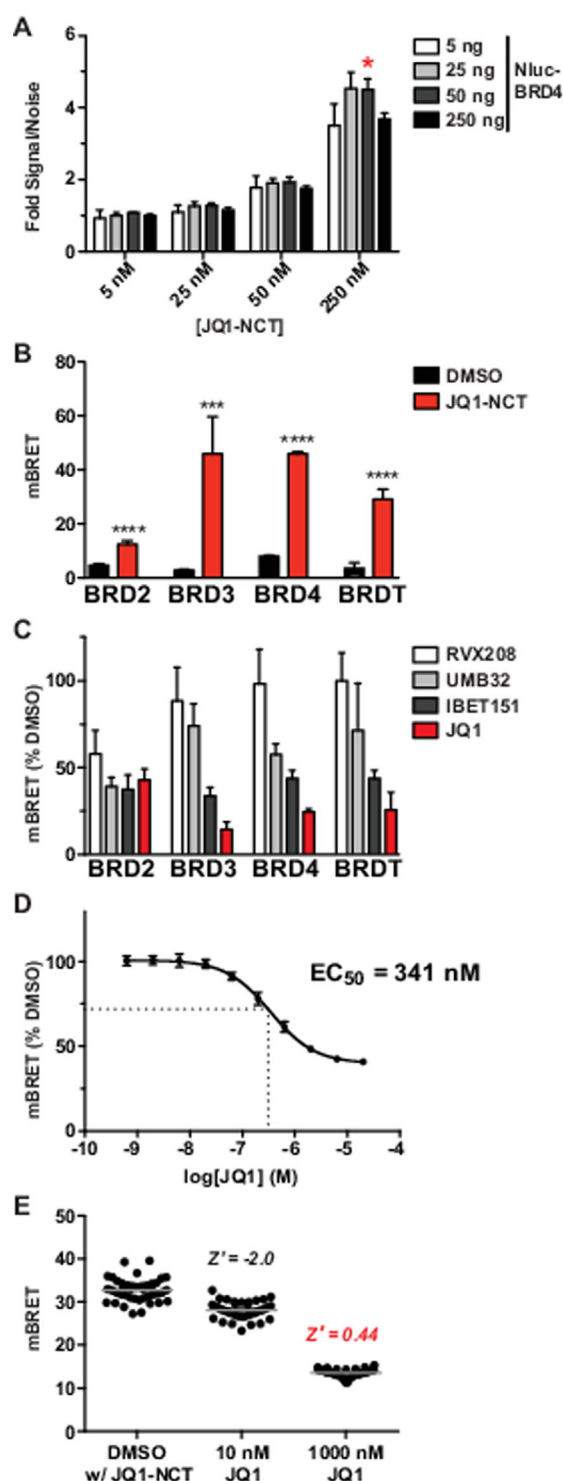
↖↖ **These are not the final page numbers!**

observed between individual BET proteins, which may reflect differences in plasmid-based expression levels between the assays, or unique cellular contexts for each BET protein. In experiments directly comparing JQ1-NCT BRET signal with that generated from BRD4–histone interactions, we observe higher signal and increased dynamic range with competitive inhibition by JQ1 using the JQ1-NCT tracer (Supporting Information Figure S1). We then evaluated the capability of BET-BRET to report on competitive inhibition of the dye-bromodomain interaction using a panel of structurally diverse BET ligands at a dose of 1 μm (RVX208, UMB32, IBET151, JQ1). Following two hours of treatment, each inhibitor displays previously reported trends of in vitro potency against the BET bromodomains; JQ1 displayed the most potent target engagement for most BETs tested, followed by the dimethyl isoxazole-based scaffolds IBET151 and UMB32 (Figure 2C).[2,5,7,9] Notably, RVX208 did not show significant target engagement in most of the assays tested, which corresponds with in vitro observations of this compound as a weak BET ligand and reveals our BET-BRET system most reliably reports on the cellular activity of compounds with sub-micromolar in vitro affinity. Robust dose–response characteristics could be obtained with inhibitor treatment and EC_{50} values that correspond to concentrations known to effect cancer cell phenotypes with longer treatment times (Figure 2D). Maximal inhibition of the assay results in a slightly greater than 50% overall signal inhibition relative to vehicle control-treated samples. This corresponds to observed dose–response characteristics of BRD4-BRET systems using histone co-expression.[10] In an effort to use BET-BRET for high-throughput assessment of larger compound libraries, we evaluated its performance in a 384-well plate format (Figure 2E). Using JQ1 as a competitive inhibitor of the assay, robust Z'-factor scores were achieved at moderate inhibitor concentrations.

While previous studies of BET inhibitors have used cellular viability assays as a high-throughput surrogate for cellular activity, this is less feasible for a recently reported class of compounds that can inhibit both BET proteins and selected kinase signaling proteins.[13–15] This includes BI2536 that possesses dual activity against BET proteins and PLK1. Each of these activities likely contributes to decreased cellular viability. Therefore, to assess the cellular inhibition of BRD4 in a high-throughput fashion, we tested BI2536 and a collection of structurally analogous derivatives predicted to be JQ1-competitive in the BET-BRET assay. These compounds included derivatives of BI2536, with varying substituents on the dihydropteridinone core and off of the central aryl ring. As shown in Figure 3A, replicate experiments are highly correlated with an R^2 value of 0.794. Compounds tested have a range of activities in the assay, including active BRD4-engaging compounds (e.g., BI2536, compound **2**), inactive compounds (e.g., compound **7**), and compounds that display apparent artefactual BRET activity. Active compounds can be seen to have dose-specific effects in the assay including BI2536 and **2** (Figure 3B). We compared data obtained from the JQ1-NCT BRET screen with biochemical AlphaScreen data in an attempt to identify interesting trends. We observed that the most potent compounds in the BET-
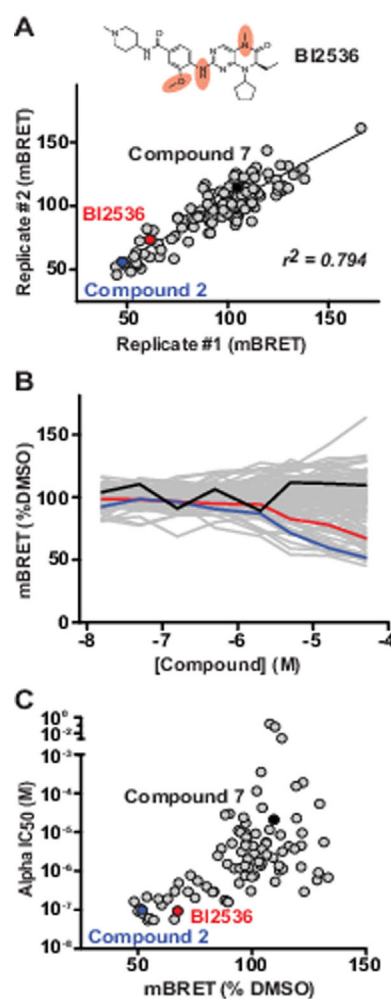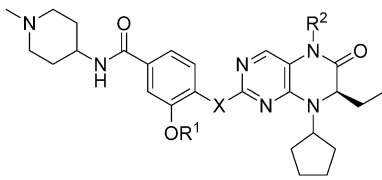

Figure 3.
A BET-BRET screen of a BI2536 scaffold library. A) Replicate concordance of two BRD4 BET-BRET assays. A 5 μm treatment of each compound was used in 384-well format ($n = 95$ compounds). BI2536 is shown along with two compounds used for further evaluation. Inset shows BI2536 structure with highlighted regions of derivatization. B) Dose–response activity of BI2536 scaffold library. Highlighted are BI2536 (red line), **2** (blue line), and **7** (black line). Data are the mean of duplicate experiments. C) mBRET signal (5 μm) versus AlphaScreen IC_{50} values for each compound tested. Highlighted are BI2536, **2**, and **7**. Shown are 92 of the 95 compounds used in the BET-BRET screen for which AlphaScreen data were available. Data are the mean of duplicate experiments.

BRET experiments also tended to display superior in vitro inhibitory activity (Figure 3C). However, some compounds that display high potency in the in vitro assay show low or minimal inhibition in the BET-BRET assay, perhaps an indication of lower cell permeability or poor stability in culture media. Thus, the paired analysis affords the ability to stratify and triage cell-active, selective BET ligands in a clear and rapid manner.

To confirm the observations made from the BET-BRET screening, we selected several compounds for further characterization by assessing PLK1 inhibitory activity and dose–response effects on viability of the MV4;11 human leukemia cell line (Table 1). Included in this set are four compounds recently described by Chen et al. in similar in vitro BRD4 and PLK1 activity and cell viability assays (**1/39 q**, **3/39 p**, **5/39 b**, **7/39 a**).[15] Our

Table 1. Structures and activities of BRD4/PLK1 inhibitors.

Compound	R^1	R^2	X	BRD4 IC$_{50}$ [nM][a]	BRET signal [%][a,b]	PLK1 IC$_{50}$ [nM][a]	MV4;11 IC$_{50}$ [nM][c]
BI2536	Me	Me	NH	142	67.5	5	4.7–6.0
1 (DB-1-205)	Me	Me	O	415	66.2	>10 000	265–377
2 (DB-1-264)	Me	Me	NMe	130	51.8	725	184–218
3 (DB-1-285)	cPent	Me	NH	112	60.4	19	65.0–78.0
4 (DB-2-011)	iPr	Me	NH	96	55.0	8	31.2–46.5
5 (DB-2-059)	Me	Et	NH	339	89.5	20	99.0–127
6 (DB-2-073)	4-(THP)	Me	NH	175	51.9	58	69.8–79.7
7 (DB-2-101)	Me	H	NH	9171	>100	129	272–337

[a] Values are the mean of duplicate measurements. [b] Treatment at 5 μM. [c] Cell viability reported as 95% confidence intervals ($n = 4$).

data here largely corresponds with previously reported activity trends for these compounds. We also included in our analysis several compounds with unique activity profiles reported for the first time here (including **2** and **7** highlighted in Figure 3). In particular we observe that **2** maintains potent BRD4 activity with decreased inhibition of PLK1 when compared with BI2536. This increased selectivity for BRD4 is due to the methylation of a key N–H with an *N*-methyl group, which forms a direct hydrogen bond with the hinge region of PLK1,[16] but establishes a weaker water-mediated hydrogen bond in crystal structures of BI2536 bound to the first bromodomain of BRD4 (BRD4-1).[13,14] The affinity of **2** for BRD4 is slightly higher than that of BI2536, and the crystal structure of **2** bound to BRD4-1 shows that the aryl ring and tail of the inhibitor is oriented differently from BI2536 (Supporting Information Figure S2), suggesting a degree of tolerance in this region (Figure 4A). An orthogonal cellular thermal shift assay (CETSA) probing for BRD4 was used to validate the cellular BET inhibitory activity of **2** (Figure 4B). Compound **2** stabilized BRD4 in cells, as did JQ1 and BI2536. Notably, **7** did not stabilize BRD4, correlating with the BET-BRET observations.

While both compounds are active in the BET-BRET assay, **2** had increased potency against BRD4 relative to BI2536. However it was far less potent in decreasing the viability of MV4;11 cells. These data suggest that the increased activity of BI2536 in MV4;11 cells is due to its effects on PLK1 inhibition rather than BRD4 inhibition. To confirm this hypothesis, we analyzed the effects of **2**, BI2536, JQ1 and the selective PLK1 inhibitor GSK461364 on the cell cycle of MV4;11 leukemia cells (Figure 4C,D). While JQ1 did not have a strong effect on cell cycle, GSK461364 induced a G$_2$M arrest. Testing each at their cellular IC$_{50}$, BI2536 induced a similar G$_2$M arrest, whereas **2** did not. These data help to confirm that the effects of BI2356 on MV4;11 viability are primarily due to PLK1 inhibition (as with GSK461364) while **2** acts as a selective BET inhibitor similar to JQ1. Thus, the BET-BRET system helps identify the pertinent intracellular targets of small molecules that lead to their broad cellular effects.

Our use of JQ1-NCT as an intracellular BRET tracer suggests it as a useful tool for the large-scale characterization of cell-active BET inhibitors. Furthermore, this approach can be used to dissect the specific activity of molecules suspected or predicted to have multiple cellular targets. Notably, similar probes have also been used to resolve intracellular residence time of ligand target engagement via dynamic monitoring of BRET signal in live cells.[12] Thus, we believe this approach is generalizable and can be applied to many protein classes amenable to Nluc tagging and anticipate this strategy will be expanded upon and improved as a tool for target-oriented chemical screening and target engagement measurements.

Experimental Section

Plasmid construction: BET family cDNAs were obtained from the Harvard Plasmid repository and were PCR-amplified with primers containing SgfI (forward) and PmeI (reverse) restriction sites. PCR products were digested using the Flexi enzyme blend (Promega). PFN31K vector (Promega) was also digested according to the Flexi digestion protocol. Ligation of the PCR products and digested PFN31K vector using T4 ligase (Promega) generated Kanamycin selectable vectors containing BET gene products with N-terminal Nanoluciferase tags. Vectors were transformed into DH5α sub-cloning efficiency *E. coli* and colonies were screened for correct DNA sequences.

96-well BET-BRET: HEK293T cells were seeded onto six-well plates at a density of 4×10^5 cells per mL, 2 mL per well. After 6 h incubation (37 °C, 5% CO$_2$) cells were transfected with 50 ng of PFN31K vectors containing BET protein cDNAs using Xfect reagent per manufacturer's protocol (Clontech). After overnight incubation, transfected cells were split using phenol-free trypsin and phenol-free DMEM (Gibco) supplemented with 10% FBS into experimental aliquots with JQ1-NCT dye and control aliquots with equal volumes of DMSO. JQ1-NCT concentration was 250 nM unless otherwise indicated. Synthesis of JQ1-NCT is described in the Supporting Information. Cells were plated onto white-bottomed 96-well plates (PerkinElmer) at a density of 10 000 cells per well with five DMSO control wells and five experimental JQ1-NCT wells per treatment. Drugs were incubated with cells for 2 h at 37 °C, 5% CO$_2$ at the in-

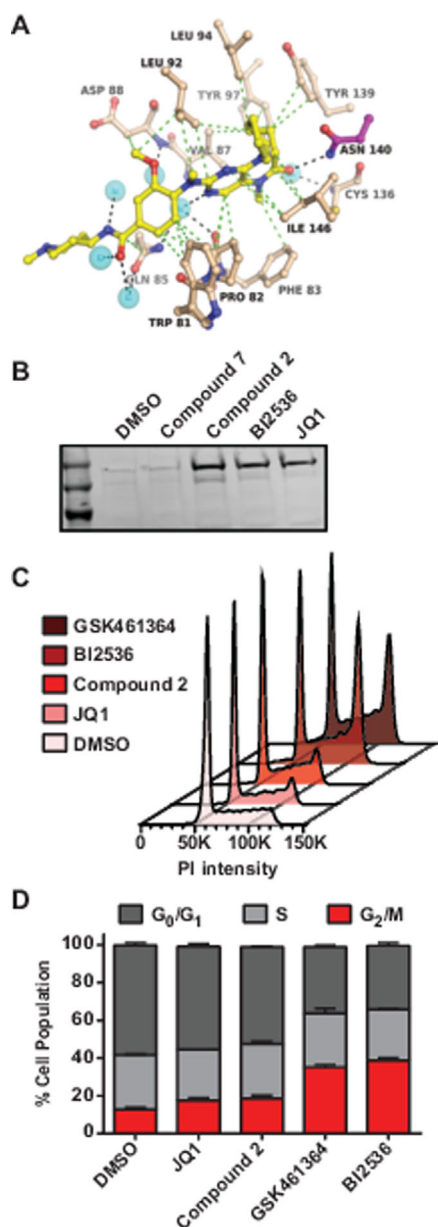↖↖ **These are not the final page numbers!**

Figure 4. Structural and cellular evaluation of BET-BRET-selected BRD4 inhibitors. A) Crystal structure of **2** in complex with BRD4 bromodomain 1. Dashed lines represent hydrogen bond interactions with BRD4 Asn140. B) CETSA analysis of compounds. MV4;11 cells were treated with JQ1, BI2536, or **2** for 3 h at 1 μM. Ladder bands represent 250 kDa (upper), 150 kDa (middle), and 100 kDa (lower) markers. C) Cell-cycle profile evaluation of MV4;11 cells treated with indicated compounds (PI = propidium iodide). D) Quantification of MV4;11 cell-cycle profiles.

dicated concentrations. Subsequently, cells were incubated with NanoGlo Luciferase Assay Substrate (Promega, 1:1000 final dilution) for 15 min at room temperature before samples were read on an Envision plate reader (PerkinElmer). Donor luminescence was read at 460 nm and acceptor fluorescence was read at 615 nm; milliBRET (mBRET) was calculated as the ratio of fluorescent to luminescent signal multiplied by 1000. The mean and standard deviation of each set of five measurements taken per sample are reported. Fold signal-to-noise ratios were calculated for each concentration of BET plasmid transfected. Signal-to-noise ratios were calculated as the ratio of the means of JQ1-NCT treated cells to

DMSO control cells. Standard deviation of signal/noise was calculated as the mean multiplied by the square root of the sum of each sample's (with and without JQ1-NCT) standard deviation divided by its mean squared. mBRET (%DMSO) was calculated as raw mBRET signal normalized to the DMSO signal for the corresponding sample [Equations (1), (2), and (3)]:

$$mBRET = \frac{Fluorescence}{Luminescence} * 1000 \tag{1}$$

$$mBRET(\% \, DMSO) = \frac{mBRET_{(Sample)}}{mBRET_{(DMSO)}} \tag{2}$$

$$StDev._{\left(\frac{Signal}{Noise}\right)} = Mean_{\left(\frac{Signal}{Noise}\right)} * \sqrt{\left(\frac{StDev._{(JQ1-NCT)}}{Mean_{(JQ1-NCT)}}\right)^2 + \left(\frac{StDev_{(DMSO)}}{Mean_{(DMSO)}}\right)^2} \tag{3}$$

384-well BET-BRET: HEK293T cells were transfected and split as described above. Cells were plated into white-bottomed 384-well plates (Nunc) at 10 000 cells per well in 50 μL final volume. Drugs were pinned into 384-well plates at the indicated final concentrations using a 100 nL pinhead on a JANUS workstation from PerkinElmer; incubation was performed as described above. NanoGlo Luciferase Assay Substrate was administered at a 1:750 final dilution. Plates were read as described above.

96-well histone-based BRET: HEK293T cells were transiently transfected with 25 ng of BRD4 PFN31K vector with N-terminally Nanoluciferase tag and 2 μg of Histone H3.3-HaloTag fusion vector (Promega). Transfected cells were split, plated, treated with JQ1, and BRET was generated using HaloTag NanoBRET ligand per manufacturer's instructions.

AlphaScreen assays: BRD4 AlphaScreen assays were conducted as described.[7] Briefly, BRD4 bromodomain (site 1) was bound to AlphaScreen emission beads via a $(His)_6$ tag. These beads were treated with compound for 1 h at room temperature. Subsequent to treatment, biotinylated-JQ1 was added to the mixture concurrently with streptavidin coated AlphaScreen donor beads. Emissions were recorded using an Envision plate reader (PerkinElmer).

Cellular viability: Cell lines were incubated with compounds for 72 h at 37 °C and ATPlite (PerkinElmer) reagent was used to assess cell viability per the manufacturer's protocol. Luminescence was read on an Envision plate reader.

Cell-cycle analysis: After treatment, cells were washed with PBS and then fixed overnight at −20 °C in 70% ethanol. Cells were washed once more with PBS and then incubated at 37 °C for 20 min in propidium iodide staining solution: 20 μg mL^{-1} propidium iodide (Life Technologies), 0.1% (v/v) Triton X-100 in PBS, supplemented with 200 μg mL^{-1} RNase A (Roche). Flow cytometry analyses were performed on a LSRFortessa X-20 flow cytometer (BD Biosciences) and all data analyzed with FlowJo software (v10, Tree Star).

BRD4 CETSA: MV4;11 cells were incubated with compounds of interest at 1 μM for 3 h at 37 °C. Following incubation, samples were centrifuged at 500 g for 3 min to pellet cellular material. Pellets were washed with 200 μL PBS and re-centrifuged; 190 μL supernatant was removed, and the remaining sample was heated at 47.5 °C for 3 min and incubated at room temperature for another 3 min. The samples were then resuspended in lysis buffer (50 mM Tris·HCl pH 7.5, 5% glycerol, 100 mM NaCl, 1.5 mM MgCl$_2$, 0.2% NP-40) supplemented with protease inhibitor cocktail and lysed by three cycles of freeze–thaw using liquid nitrogen. Lysed samples

These are not the final page numbers! ↗↗

were then spun at 20 000 *g* for 20 min at 4 °C to pellet; 30 µL supernatant were mixed with gel loading buffer and the gel was run using BOLT running conditions (Thermo Fisher). Blots were then transferred with the iBLOT transfer station, blocked for 1 h at room temperature using Odyssey blocking buffer, and developed using an anti-BRD4 antibody (Bethyl). A LICOR gel visualizing system was used for imaging the blots.

PLK1 activity assay: The enzymatic activities against PLK1 were tested in Z-Lyte assays with ATP concentrations of K_M for each kinase per manufacturer's protocol (Thermo Fisher).

Characterization of JQ1-NCT probe: Fluorescent and luminescent characterization of JQ1-TOM probe was done using a TECAN SAFIRE II plate reader using a 5 µm solution resuspended in PBS. Fluorescence excitation scanning was conducted between wavelengths 500 nm to 650 nm with a 1 nm wavelength step size and emission readings beginning at 690 nm; gain was set to 140. Absorbance parameters were obtained by scanning with an excitation wavelength beginning at 550 nm and a scanning window for emission from 600 nm to 800 nm. A 1 nm step size was used with gain set to 140.

X-ray crystallography: Reagents and compounds for crystallographic experiments were purchased from Hampton Research unless otherwise indicated. BRD4-1 was purified as described previously.[14] Crystals of BRD4-1 were grown by vapor-diffusion in hanging drops using 0.2 M $(NH_4)_2SO_4$, 0.1 M Tris·HCl (pH 8.5) and 25 % (w/v) PEG 3350 as precipitant supplemented with 1 mm DB-1-264-2 and 10 % (v/v) DMSO.[14] Crystals were harvested in cryoprotectant (three parts precipitant including 0.5 mM DB-1-264-2 and one part 100 % (v/v) ethylene glycol) and flash frozen in a stream of nitrogen gas. X-ray diffraction data were recorded at −180 °C using $Cu_{K\alpha}$ X-rays produced by a Rigaku Micro-Max 007-HF X-ray generator, focused by mirror optics and equipped with a Rigaku CCD Saturn 944 system. Data were reduced and scaled with XDS.[17] PHENIX was employed for phasing and refinement, and model building was performed using Coot.[18, 19] The structure was solved by molecular replacement using Phaser with the monomer of PDB ID: 4O7A as the search model.[20] An initial model of the inhibitor was generated using MarvinSketch (ChemAxon) with ligand restraints from eLBOW of the PHENIX suite. All structures were validated by MolProbity and phenix.model_vs_data.[21,22] Figure were prepared using PyMOL (Schrödinger). Atomic coordinates and structure factors have been deposited in the Protein Data Bank (PDB) under accession code 5KJ0.

Acknowledgements

Keywords: bromodomain inhibition · drug design · epigenetics · fluorescence · in-cell target engagement assays · luminescence

[1] P. Filippakopoulos, S. Knapp, *Nat. Rev. Drug Discovery* **2014**, *13*, 337–356.

[2] P. Filippakopoulos, J. Qi, S. Picaud, Y. Shen, W. B. Smith, O. Fedorov, E. M. Morse, T. Keates, T. T. Hickman, I. Felletar, M. Philpott, S. Munro, M. R. McKeown, Y. Wang, A. L. Christie, N. West, M. J. Cameron, B. Schwartz, T. D. Heightman, N. La Thangue, C. A. French, O. Wiest, A. L. Kung, S. Knapp, J. E. Bradner, *Nature* **2010**, *468*, 1067–1073.

[3] J. Zuber, J. Shi, E. Wang, A. R. Rappaport, H. Herrmann, E. A. Sison, D. Magoon, J. Qi, K. Blatt, M. Wunderlich, M. J. Taylor, C. Johns, A. Chicas, J. C. Mulloy, S. C. Kogan, P. Brown, P. Valent, J. E. Bradner, S. W. Lowe, C. R. Vakoc, *Nature* **2011**, *478*, 524–528.

[4] E. Nicodeme, K. L. Jeffrey, U. Schaefer, S. Beinke, S. Dewell, C.-W. Chung, R. Chandwani, I. Marazzi, P. Wilson, H. Coste, J. White, J. Kirilovsky, C. M. Rice, J. M. Lora, R. K. Prinjha, K. Lee, A. Tarakhovsky, *Nature* **2010**, *468*, 1119–1123.

[5] M. A. Dawson, R. K. Prinjha, A. Dittmann, G. Giotopoulos, M. Bantscheff, W.-I. Chan, S. C. Robson, C.-W. Chung, C. Hopf, M. M. Savitski et al., *Nature* **2011**, *478*, 529–533.

[6] S. Picaud, D. Da Costa, A. Thanasopoulou, P. Filippakopoulos, P. V. Fish, M. Philpott, O. Fedorov, P. Brennan, M. E. Bunnage, D. R. Owen, J. E. Bradner, P. Taniere, B. O'Sullivan, S. Müller, J. Schwaller, T. Stankovic, S. Knapp, *Cancer Res.* **2013**, *73*, 3336–3346.

[7] M. R. McKeown, D. L. Shaw, H. Fu, S. Liu, X. Xu, J. J. Marineau, Y. Huang, X. Zhang, D. L. Buckley, A. Kadam, Z. Zhang, S. C. Blacklow, J. Qi, W. Zhang, J. E. Bradner, *J. Med. Chem.* **2014**, *57*, 9019–9027.

[8] G. Zhang, S. G. Smith, M.-M. Zhou, *Chem. Rev.* **2015**, *115*, 11625–11668.

[9] S. Picaud, C. Wells, I. Felletar, D. Brotherton, S. Martin, P. Savitsky, B. Diez-Dacal, M. Philpott, C. Bountra, H. Lingard, O. Fedorov, S. Müller, P. E. Brennan, S. Knapp, P. Filippakopoulos, *Proc. Natl. Acad. Sci. USA* **2013**, *110*, 19754–19759.

[10] T. Machleidt, C. C. Woodroofe, M. K. Schwinn, J. Méndez, M. B. Robers, K. Zimmerman, P. Otto, D. L. Daniels, T. A. Kirkland, K. V. Wood, *ACS Chem. Biol.* **2015**, *10*, 1797–1804.

[11] T. A. Kirkland, M. G. McDougall, S. Dwight (Promega Corporation, Madison, WI) Int. PCT Pub. No. WO2013078244, **2013**.

[12] M. B. Robers, M. L. Dart, C. C. Woodroofe, C. A. Zimprich, T. A. Kirkland, T. Machleidt, K. R. Kupcho, S. Levin, J. R. Hartnett, K. Zimmerman, A. L. Niles, R. F. Ohana, D. L. Daniels, M. Slater, M. G. Wood, M. Cong, Y.-Q. Cheng, K. V. Wood, *Nat. Commun.* **2015**, *6*, 10091.

[13] P. Ciceri, S. Müller, A. O'Mahony, O. Fedorov, P. Filippakopoulos, J. P. Hunt, E. A. Lasater, G. Pallares, S. Picaud, C. Wells, S. Martin, L. M. Wodicka, N. P. Shah, D. K. Treiber, S. Knapp, *Nat. Chem. Biol.* **2014**, *10*, 305–312.

[14] S. W. J. Ember, J.-Y. Zhu, S. H. Olesen, M. P. Martin, A. Becker, N. Berndt, G. I. Georg, E. Schönbrunn, *ACS Chem. Biol.* **2014**, *9*, 1160–1171.

[15] L. Chen, J. L. Yap, M. Yoshioka, M. E. Lanning, R. N. Fountain, M. Raje, J. A. Scheenstra, J. W. Strovel, S. Fletcher, *ACS Med. Chem. Lett.* **2015**, *6*, 764–769.

[16] M. Kothe, D. Kohls, S. Low, R. Coli, G. R. Rennie, F. Feru, C. Kuhn, Y.-H. Ding, *Chem. Biol. Drug Des.* **2007**, *70*, 540–546.

[17] W. Kabsch, *Acta Crystallogr. Sect. D* **2010**, *66*, 125–132.

[18] P. D. Adams, P. V. Afonine, G. Bunkóczi, V. B. Chen, I. W. Davis, N. Echols, J. J. Headd, L.-W. Hung, G. J. Kapral, R. W. Grosse-Kunstleve, A. J. McCoy, N. W. Moriarty, R. Oeffner, R. J. Read, D. C. Richardson, J. S. Richardson, T. C. Terwilliger, P. H. Zwart, *Acta Crystallogr. Sect. D* **2010**, *66*, 213–221.

🢨🢨 **These are not the final page numbers!**

[19] P. Emsley, B. Lohkamp, W. G. Scott, K. Cowtan, *Acta Crystallogr. Sect. D* **2010**, *66*, 486–501.

[20] A. J. McCoy, R. W. Grosse-Kunstleve, P. D. Adams, M. D. Winn, L. C. Storoni, R. J. Read, *J. Appl. Crystallogr.* **2007**, *40*, 658–674.

[21] V. B. Chen, W. B. Arendall, J. J. Headd, D. A. Keedy, R. M. Immormino, G. J. Kapral, L. W. Murray, J. S. Richardson, D. C. Richardson, *Acta Crystallogr. Sect. D* **2010**, *66*, 12–21.

[22] P. V. Afonine, R. W. Grosse-Kunstleve, V. B. Chen, J. J. Headd, N. W. Moriarty, J. S. Richardson, D. C. Richardson, A. Urzhumtsev, P. H. Zwart, P. D. Adams, *J. Appl. Crystallogr.* **2010**, *43*, 669–676.
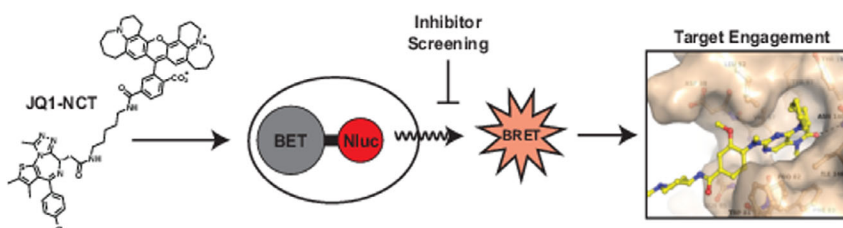
These are not the final page numbers! ↗↗

COMMUNICATIONS

*L. W. Koblan, D. L. Buckley, C. J. Ott,
M. E. Fitzgerald, S. W. J. Ember, J.-Y. Zhu,
S. Liu, J. M. Roberts, D. Remillard,
S. Vittori, W. Zhang, E. Schonbrunn,
J. E. Bradner**

■■ – ■■

Assessment of Bromodomain Target Engagement by a Series of BI2536 Analogues with Miniaturized BET-BRET

Place your BETs on BRET: Target engagement assays for evaluating small molecules in cells provide valuable information for the development of drugs and probes. Here, a high-throughput bioluminescence resonance energy transfer assay is used to study bromo- domain inhibition. Novel bromodomain-specific inhibitors are identified from a series of bromodomain- and kinase-binding polypharmacophores whose cellular activity can obscure the pertinent biological target of the compounds.

↖↖ **These are not the final page numbers!**